

Numerical modelling of natural convection of oil inside distribution transformers

Abbreviated title: Numerical thermal model of distribution transformers

Jon Gastelurrutia^{a,*}, Juan Carlos Ramos^a, Gorka S. Larraona^a, Alejandro Rivas^a, Josu Izagirre^b and Luis del Río^b

^a *TECNUN (University of Navarra) – Dept. of Mech. Engineering, Thermal and Fluids Engineering Div. Paseo de Manuel de Lardizábal 13, 20018 San Sebastián, Spain*

^b *O.C.T. (Ormazabal Corporate Technology) Parque Empresarial Boroa, 48340 Amorebieta-Etxano, Spain*

Abstract

The thermal behaviour of several ONAN (Oil Natural – Air Natural) distribution transformers has been numerically modelled. Based on the results of a previous complete model, a simplified differential model has been developed with the aim of reducing the computational cost. This model has been capable of reproducing, with acceptable accuracy, the oil flow and the thermal distribution inside the transformer. The influence of turbulence modelling in the obtained results has been evaluated and the model has been verified in terms of discretization errors. The thermal boundary conditions have been thoroughly analysed searching for the most appropriate expressions for this particular case instead of using inadequate mean values obtained from bibliography. The devised model has been validated by comparing the numerical results with the experimental ones obtained for different transformers and power losses. This mathematical tool can be used to study the natural convection of the oil inside the transformers and allows the manufacturers to optimise their designs from a thermal point of view.

Keywords: thermal modelling, natural convection, *CFD*, distribution transformer.

Nomenclature

Latin Letters

A	surface area, [m ²]
L	characteristic length, [m]
Nu_L	Nusselt number, [-]
Nu_y	local Nusselt number, [-]
P	static pressure, [Pa]
P_N	measured power loss, [W]

Pr_T	turbulent Prandtl number, [-]
Ra_L	Rayleigh number, [-]
Ra_y	local Rayleigh number, [-]
T	temperature, [K or °C]
T_{amb}	ambient temperature, [K or °C]
T_f	film temperature, [K or °C]
T_{rad}	black body temperature, [K or °C]
T_{ref}	reference temperature, [K or °C]
T_s	surface temperature, [K or °C]
$T_{s,y}$	local surface temperature, [K or °C]
U_i	velocity components, [m/s]
Vol	volume of copper, [m ³]
c_p	specific heat, [J/kg·K]
g	gravity acceleration, [m/s ²]
h	heat transfer coefficient, [W/m ² ·K]
h_y	local heat transfer coefficient, [W/m ² ·K]
k	turbulent kinetic energy, [m ² /s ²]
q''	heat flux, [W/m ²]
x_i	Cartesian coordinates, [m]
y	local vertical coordinate, [m]

Greek Letters

α	thermal diffusivity, [m ² /s]
β	thermal expansion coefficient, [1/K]
δ_{ij}	Kronecker delta, [-]
ε	dissipation rate of k , [m ² /s ³]
λ	thermal molecular conductivity, [W/m·K]
λ_T	turbulent thermal diffusivity, [W/m·K]
μ	dynamic molecular viscosity, [kg/m·s]

μ_T	turbulent eddy viscosity, [kg/m·s]
ν	kinematic molecular viscosity, [m ² /s]
ρ	density, [kg/m ³]
ρ_o	reference density, [kg/m ³]

1. INTRODUCTION

A wide variety of *ONAN* cooled distribution transformers is commonly used in electrical power delivery networks. The purpose of this kind of transformer is to convert distributed electrical energy from medium voltage to low voltage for domestic and industrial applications. In this conversion there are some power losses that are transformed into heat inside the transformer. An unsuitable dissipation of this heat can lead to an excessive increase in the “hot-spot” temperature in the inner part of the coils that could cause a premature ageing of the transformer, malfunctions, or even accidents involving fire [1]. For these reasons, optimal design of transformers with respect to cooling is necessary in order to avoid faulty operation and material degradation due to thermal damage. Therefore, the basic methodology to characterise the thermal performance of a distribution transformer working in open air conditions is usually based on the experimental heating tests and on the simplified calculation methods specified by International Standards [2, 3].

Looking for a more comprehensive thermal characterization, several authors have studied the performance of transformers by means of simplified equivalent thermal circuits using different approaches [4-9]. These models are based on a short number of characteristic temperatures inside the transformer and they rely on some coefficients whose values have to be determined by means of experimentation for each new design. A common characteristic of these “network models” is that they can be used to determine load capability and ageing of a specific and experimentally checked system using discrete temperature measurements, but not to obtain an optimal design.

So, in order to deal with design and optimisation objectives, the use of other types of mathematical models with a more exhaustive treatment of the physical phenomena that is taking place in the transformer is required. Several studies have also been carried out in that direction, developing models of different types of transformers and solving them numerically. For example, in [10], Oh and Ha analysed

the turbulent natural convection of oil inside a cylindrical single-phase transformer using a specific Low-Reynolds Number turbulence model. Although it was a 3D model, a lot of geometry simplifications were assumed and uniform temperatures were imposed as boundary conditions. Mufuta and Van den Bulck [11] focused on the laminar mixed oil convection (natural and forced) inside the vertical and horizontal channels of a disc-type power transformer, proposing a general heat transfer coefficient dependent on different modelled parameters. For simplicity, a 2D axisymmetrical model was used to represent one of the coils of the three-phase power transformer assuming equal performance in each of them.

In this paper, a simplified mathematical model based on the differential description of the oil flow and the heat transfer inside *ONAN* distribution transformers is presented in conjunction with the numerical procedure to solve it. A lot of computational resources will be saved taking into account the proposed simplifications, especially the reduction of the oil flow domain to a perpendicular cut or slice of the complete transformer. The performance in open air conditions is going to be studied, and the thermal boundary conditions are going to be thoroughly analysed to search for a simple and functional characterisation. After checking equivalent internal oil flow and thermal performances in comparison with those provided by a more detailed complete model, the results of the devised model have been validated using experimental surface temperature measurements. Using the model, a description of the main features of the natural convection oil movement inside distribution transformers can be ascertained. This information will be used in future works to build a simplified algebraic zonal model of the transformer cooling which will demand lower computational resources and will be easier to implement in design-oriented software.

2. DESCRIPTION OF *ONAN* DISTRIBUTION TRANSFORMERS

Figure 1 shows internal and external views of the reference three-phase distribution transformer identified as *Transf-01* which has been modelled in the present paper. The input voltage during the standard performance of the transformer is 25 kV at 50 Hz and it handles 630 kVA. The total height of the external casing, $H_{casing,1}$, is 1005 mm, the longest horizontal side, $L_{casing,1}$, measures 1275 mm, and the shortest side, $W_{casing,1}$, is 500 mm. The number of fins, $N_{fins,1}$, is 64 and their dimensions are a height of 800 mm, $H_{fins,1}$, and a length of 230 mm, $L_{fins,1}$. The total weight when the transformer is filled with oil is close to 2000 kg. The performance of two additional similar transformers, *Transf-02* and *Transf-03*, are

going to be analysed in the last part of the paper. As can be seen in Table 1, *Transf-02* is smaller than *Transf-01* but it contains more external fins; on the contrary, *Transf-03* is slightly bigger and has more and longer fins.

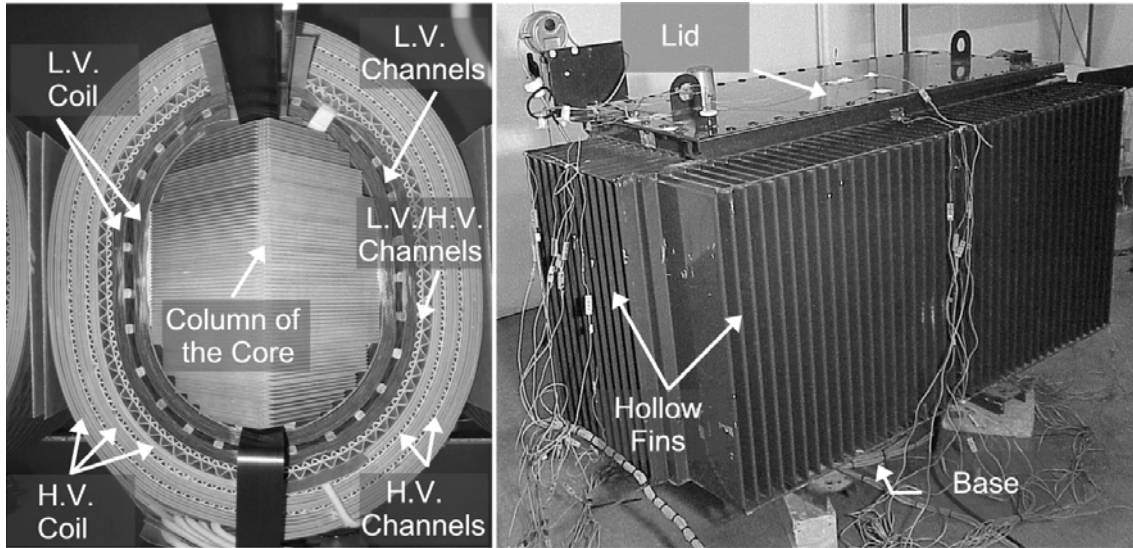


Figure 1 Different views of *Transf-01* with its main components: Internal view (left), External view (right).

The internal components of the transformer are the core and the coils. The ferromagnetic core consists of piled up laminated steel sheets forming a structure of three columns joined by two horizontal beams at the top and the bottom parts of the columns. Around each of the three columns of the core, the coils or windings are arranged as shown in Fig. 1 (left). The windings are made of alternative layers of copper and insulating paper. These internal components are the transformer's heat generation sources due to power losses. There are two types of power losses: the magnetic or no-load losses that take place at the core, and the copper or load losses that happen in the coils [1]. In the case of *Transf-01* the total power losses $P_{N,1}$ are 8100 W, with a measured distribution of 17.9% in the core and 82.1% in the coils. As can be seen in Table 1, *Transf-02* generates less power losses than *Transf-01*; on the contrary, the bigger *Transf-03* generates higher power losses.

It has been highlighted in Fig. 1 (left) that the coils have a vertical channel configuration in order to ensure dielectric insulation between the low voltage (LV) and the high voltage (HV) sides and a proper cooling for the entire set. In the case of transformer *Transf-01*, there is a set of vertical channels with a rectangular cross-section in the LV windings and there are two sets of vertical channels with a triangular

cross-section in the HV windings. A double set of triangular vertical channels separates both electrical sides. The importance of this kind of cooling channel has been highlighted by several authors [11, 12].

Table 1 Main characteristic of the analysed commercial *ONAN* distribution transformers.

	<i>Transf-02</i>	<i>Transf-03</i>
P_N (W)	$0.82 \cdot P_{N,1}$	$1.53 \cdot P_{N,1}$
W_{casing} (mm)	$1 \cdot W_{casing,1}$	$1.08 \cdot W_{casing,1}$
L_{casing} (mm)	$0.86 \cdot L_{casing,1}$	$0.96 \cdot L_{casing,1}$
H_{casing} (mm)	$0.92 \cdot H_{casing,1}$	$0.97 \cdot H_{casing,1}$
H_{fins} (mm)	$0.88 \cdot H_{fins,1}$	$0.88 \cdot H_{fins,1}$
L_{fins} (mm)	$0.87 \cdot L_{fins,1}$	$1.35 \cdot L_{fins,1}$
N_{fins} (units)	$N_{fins,1}+14$	$N_{fins,1}+20$

The core and the coils are introduced into the casing of the transformer that is filled with oil with suitable dielectric and thermal properties. The main purpose of the oil is to provide electric insulation and to transfer the heat generated in the internal components of the transformer to the external surfaces. As can be seen in Fig. 1 (right), surrounding the casing there is an arrangement of hollow fins to increase the effective heat dissipation area. The circulation of the oil inside the hollow fins makes them much more effective at dissipating heat than some solid fins, because the equivalent heat transfer coefficient is significantly augmented [13]. The heat is dissipated from the outer surface of the transformer by natural convection with the external air and by radiation exchanges with the surroundings.

3. EXPERIMENTAL MEASUREMENTS

Experimental measurements are needed in order to have better knowledge of the external thermal conditions and to analyse the validity of the developed model. Five different heating tests, under the regulations of International Standard IEC 60076-7 [1], have been carried out for the three transformers with different power losses as can be seen in Table 2. The building where the experimental tests have been carried out is big enough to avoid any thermal air stratification. So, all the limits of the cavity are roughly at ambient temperature. K-type thermocouples have been employed to measure temperatures in strategically situated points on the external surface of the transformer as can be seen in Figure 2. The accuracy of this kind of probe is ± 1 K. Taking into account the criteria defined to establish the end of a heating test in [1], time averaged values (obtained every hour) for both oil temperature and total power loss values have been checked and recorded. The uncertainty in the power measurement due to electrical

instability during all the tests has been estimated as $\pm 6.5\%$ for the worst case based on a *Gaussian* distribution with a confidence interval of 95% [14]. Besides, the uncertainty in the temperature measurements has been estimated to be ± 1.5 K in the worst case using the data recorded only after the stabilisation. This estimation with a small number of samples (4) is based on a *Student-t* distribution with a confidence interval of 95% [14].

Table 2 Principal experimental temperature measurements.

	<i>Transf-01</i>			<i>Transf-02</i>	<i>Transf-03</i>
	$P_{N,1}$ ^(a)	$\frac{3}{4} P_{N,1}$	$\frac{1}{2} P_{N,1}$	$P_{N,2}$ ^(b)	$P_{N,3}$ ^(c)
$T_{ambient}$ (°C)	24.8	24.2	22.9	22.0	14.6
$\Delta T_{fin\ outlet}$ (°C)	22.3	17.0	12.4	-	-
ΔT_{oil} (°C)	51.4	41.8	31.5	46.6	56.2
ΔT_1 (°C)	46.8	38.3	29.4	46.1	53.6
ΔT_9 (°C)	49.5	40.5	30.5	46.9	54.5
ΔT_{10} (°C)	47.1	38.6	28.9	44.5	49.5
ΔT_{11} (°C)	44.8	36.4	26.9	43.1	44.8
ΔT_{12} (°C)	44.4	36	26.7	42	43.9
ΔT_{13} (°C)	35.8	28.6	20.3	31.7	34.9
ΔT_{14} (°C)	34.2	27.2	19.6	30.7	32.6
ΔT_7 (°C)	13.2	11.2	8.4	17.7	18.4

(a) $P_{N,1}$ means nominal power losses under normal operating conditions for *Transf-01*.

(b) $P_{N,2}$ means nominal power losses under normal operating conditions for *Transf-02*.

(c) $P_{N,3}$ means nominal power losses under normal operating conditions for *Transf-03*.

Some of the most relevant values obtained can be seen in Table 2. Temperature increases with respect to the ambient temperature are shown in all the tables in order to have comparable values. Thermocouples were protected against radiation to avoid any undesired influence that could distort measured values, and when ambient temperatures were measured they were placed inside glass recipients filled with oil, ensuring the thermal stability of the measured value. Four different thermocouples have been used to obtain a representative mean ambient temperature. Additional air temperatures have been checked at the inlet and outlet of the fins of the short and long sides of the transformer as shown in Fig. 2. Thirty six more thermocouples were used to measure surface temperatures in an attempt to cover all the relevant parts of the transformer. The last thermocouple was used to measure an internal oil temperature at the upper part of the transformer. This top oil temperature value is used by the manufacturer to check the validity of a specific distribution transformer [2, 3].

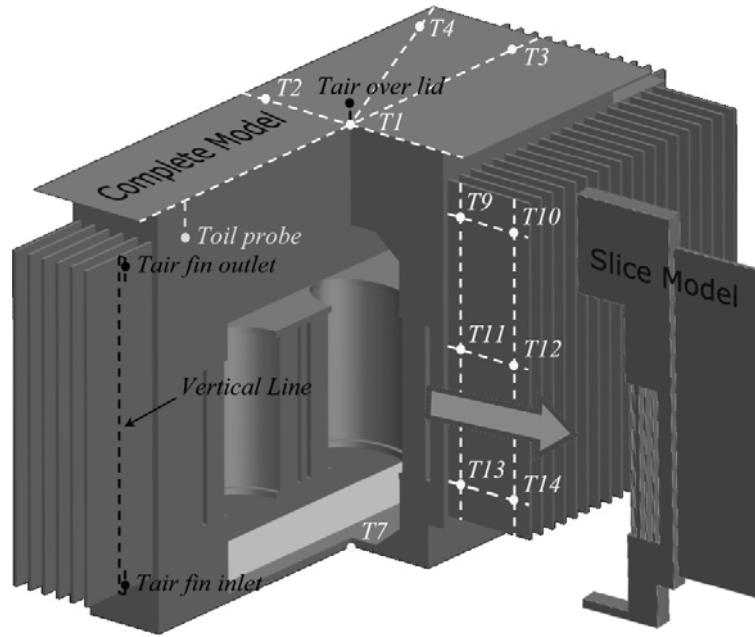


Figure 2 Position of the thermocouples during the experimental tests and geometry of the Complete and Slice Model.

Many interesting characteristics that will be reflected in the developed model can be extrapolated by evaluating the measured temperature values. It is worth highlighting that the hottest surface temperature is on the upper internal part of the fins, not on the lid, and that the base of the transformer is the coldest zone of the entire domain. Surface thermal variations on the fins are larger in the vertical direction (14 K) than in the horizontal one (2.5 K) due to the thermal stratification of the oil inside the hollow fins.

4. MATHEMATICAL MODEL

The natural convection of oil inside the described distribution transformers can be studied solving the governing differential equations restricted to the boundary conditions inside the modelled flow domain. Two different domains have been developed to study the oil flow and the heat transfer that take place in the cooling of a transformer: a Complete and a Slice domain. Although the Complete model will be used only to check the adequateness of the oil flow and thermal distribution of the Slice model, all the main characteristics of both domains, in conjunction with the applied mathematical model, will be pointed out in the following sections, paying special attention to the description of the thermal boundary conditions and their influence.

4.1. Formulation of the Problem

Developing a complete mathematical model of the transformer cooling, including the entire geometry together with the internal solid parts, the oil and the air zones, will not be an easy task. It implies enormous computational requirements and several numerical difficulties may arise. In this paper, an approach to the problem assuming some advantageous simplifications is proposed in order to reach a compromise between the accuracy of the obtained results and the required computational costs. The first simplification suggested is to reduce the domain of the model to a slice of the transformer as seen in Figure 2. Computational and time requirements are considerably reduced without losing any essential flow features. The second one is not to model the anisotropic heat conduction inside the core and the coils. In fact, no internal solid parts are included in the model, considering uniform heat fluxes for each surface of the core, the LV and HV coils. The last approximation is the use and calibration of correlations for the convective heat transfer on the external surfaces of the model, and a simplified treatment of the radiation heat exchanges. All these characteristics are fully explained and justified in the following sections.

4.2. Governing Equations

Some previous analytical estimations of the Ra number were made in order to know the most suitable flow regime for the entire domain. These numbers indicate the existence of a turbulent regime of the flow in the zone between the lid and the upper part of the core, and subsequent simulations confirmed the validity of this supposition. Taking the above into account, the *Reynolds Average* approach of the *Navier-Stokes (RANS)* equations, (1) and (2), and the Energy equation (3) is used to include turbulence effects in the mean flow variables. The buoyancy term has been included in the right side of equation (2) to take into account the movement provoked by density variations of the oil.

This density is assumed to vary linearly with temperature, other properties (like molecular viscosity and specific heat) are also temperature dependent and the thermal conductivity has been considered as a constant value. To be taken as a reference, the oil manufacturer indicates a value of 892 kg/m³ for the density, 0.021 kg/m·s for the dynamic viscosity, 1900 J/kg·K for the specific heat and 0.139 W/m·K for the thermal conductivity at a constant temperature of 25 °C.

$$\frac{\partial}{\partial x_i}(\rho \cdot U_i) = 0 \quad (1)$$

$$\frac{\partial}{\partial x_j}(\rho \cdot U_i \cdot U_j) = -\frac{\partial P}{\partial x_i} + \frac{\partial}{\partial x_j} \left[(\mu + \mu_T) \cdot \left(\frac{\partial U_i}{\partial x_j} + \frac{\partial U_j}{\partial x_i} \right) - \frac{2}{3} \cdot \rho \cdot k \cdot \delta_{ij} \right] - g_i \cdot (\rho - \rho_0) \quad (2)$$

$$\frac{\partial}{\partial x_i}(\rho \cdot U_i \cdot c_p \cdot T) = \frac{\partial}{\partial x_i} \left[(\lambda + \lambda_T) \cdot \frac{\partial T}{\partial x_i} \right] \quad (3)$$

Turbulence is modelled using the *RNG k-ε* turbulence model which introduces two additional equations, one for the turbulent kinetic energy and other one for its dissipation rate [15]. A *2-Layer* approach has been adopted to deal with turbulence near the walls [16]. The turbulent eddy and thermal diffusivity are calculated solving eqs. (4), with a constant value of $C_v = 100$, and (5), with a constant value of $Pr_T = 0.85$, respectively:

$$\mu_T = \mu \cdot \left[1 + \sqrt{\frac{\rho \cdot C_v}{\mu} \cdot \frac{k}{\sqrt{\varepsilon}}} \right]^2 \quad (4)$$

$$\lambda_T = \frac{c_p \cdot \mu_T}{Pr_T} \quad (5)$$

4.3. Flow Domain

Only the space occupied by the oil is considered in the developed mathematical model leaving aside the external air and the internal solid parts. The flow domains of the Complete (left) and Slice (right) models of the transformer *Transf-02* are shown in Figure 3, identifying the principal boundary limits. The internal and external geometry of both domains is equal to that found in the real transformer that they represent (see Table 1 for more details).

The Complete model has been built reproducing all the important geometrical and constructive particularities of the real transformer because its main function is to provide a realistic idea of the 3D oil movement and thermal distribution inside the transformer. Nevertheless, the different vertical cooling channels located in the middle of the coils have been simplified using a unique equivalent porous zone that can be seen in Fig. 3 (left) and whose characteristics will be pointed out later. In this porous media model the solid part would represent the copper that is located between channels and the porosity would represent the channels in that direction. This is done in order to reduce the number and the distortion of the cells of the Complete model.

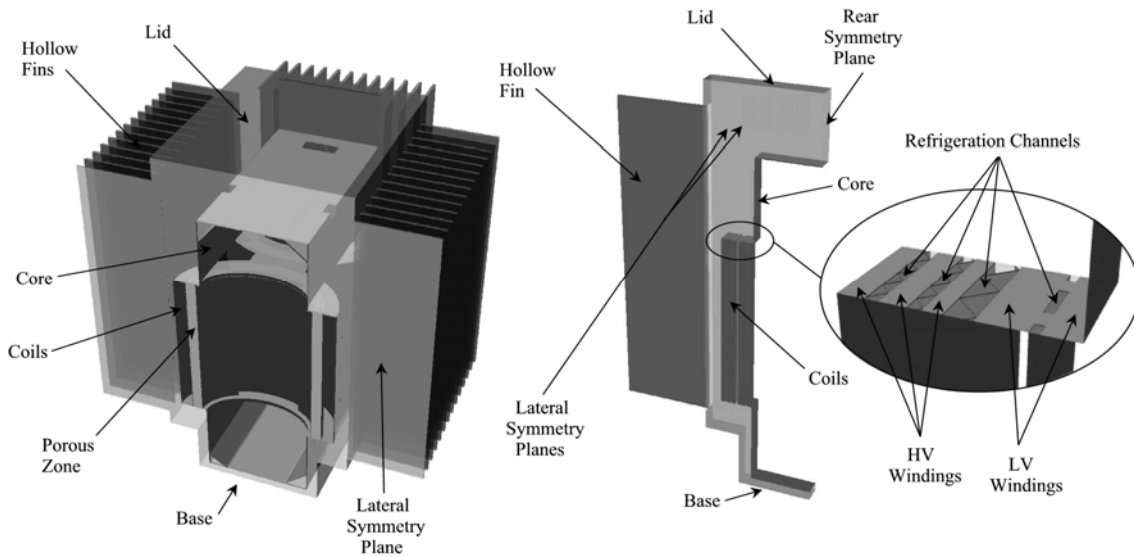


Figure 3 Developed flow domains for *Transf-02*: Complete (left), Slice (right).

The Slice model only covers the fluid that is confined in a vertical cut of the real transformer as it is schematically shown in Fig. 2. This is done by means of a couple of symmetry planes, each of them located in the middle between two consecutive fins of the longest side (L_{casing}) of the transformer. Following this, the thickness of the Slice model is equal to the separation between fins in the arrangement (this value is of 39-40 mm for all the analysed transformers). Only a unique fin filled with oil is included using another symmetry plane which is normal to the previous, reducing additionally the required domain ($W_{casing} / 2$). The height of the Slice model (H_{casing}) and all the remaining external dimensions are the same than in the real transformer. Internally, it has been considered that the Slice model is centred with respect to the winding that is located on the middle column of the tri-phase core. The cooling channels that are located separating the different zones of LV and HV coils have been modelled in a realistic way, including the corrugated cardboard placed inside, as it can be seen augmented in Fig. 3 (right). These channels are filled up with oil while the core and the different parts of the coils are represented only by their external surfaces. This is because the heat transfer inside the internal solid parts hasn't been modelled. The slight curvature of the core and the coils has been simplified using straight zones.

A high quality hexahedral mesh has been used in the discretization of both models. The number of cells in the Slice model is of the order of $1.25 \cdot 10^6$. In the Complete model the cell requirement is considerably higher and a number of $4.5 \cdot 10^6$ elements has been considered. The smaller size of the Slice domain presents the possibility of additional re-meshing stages for a grid independency analysis and

higher efficiency. The resolution of the mesh is higher in the near wall region so as to capture the larger magnitude gradients that take place there. Special care is taken as well while meshing the hollow fins and the cooling channels. All this modularity and meshing quality is achieved through the use of a non-conformal grid type, splitting the meshed domain into different coupled zones. This meshing strategy is numerically possible due to the use of a code developed explicitly for unstructured meshes [17].

4.4. Boundary Conditions

The flow and thermal boundary conditions that are needed for the oil at the limits of the proposed Complete and Slice domains are reported in Table 3 with reference to Fig. 3. A non-slip condition is ascribed to fluid velocity at all the internal and external solid walls, and the shear stress is calculated considering smooth surfaces. The normal velocity component and the normal gradients of all the other variables were set to zero at the different planes of symmetry.

Table 3 Flow and thermal boundary conditions.

Boundary Conditions				
Zone	Velocities		Thermal	
<i>Core</i>	$U_i = 0$		Unif. Heat Flux	Eq. (6)
<i>LV Coils ($Vol_{i,LV}$)</i>	$U_i = 0$		Unif. Heat Flux	Eq. (7)
<i>HV Coils ($Vol_{i,HV}$)</i>	$U_i = 0$		Unif. Heat Flux	Eq. (8)
<i>Corrugated Cardboard</i>	$U_i = 0$		Coupled	$q'' = -\lambda \cdot \frac{\partial T}{\partial x_{Normal}}$
<i>Symmetry Planes</i>	$U_{Normal} = 0$	$\frac{\partial U_i}{\partial x_{Normal}} = 0$	Adiabatic	$\frac{\partial T}{\partial x_{Normal}} = 0$
<i>Lid</i>	$U_i = 0$		Unif. Conv. + Rad.	Eqs. (10-11)
<i>Base</i>	$U_i = 0$		Unif. Conv. + Rad.	Eq. (12)
<i>Vertical (Fins)</i>	$U_i = 0$		Local Conv.	Eq. (13)

Although a specific section is later dedicated to the widening and analysis of the thermal boundary conditions, a general overview is now brought forward based on the information provided by Table 3. In this sense, uniform heat fluxes are imposed in all the internal surfaces of both models (external surfaces of the core, the LV and HV coils). As the Slice model only contains a small fraction of the Complete domain (including the core and the coil surfaces) only the corresponding fraction of the total power losses are considered in this model. Equivalent porosity, volumetric heat generation, and viscous resistances are imposed in the porous region of the Complete model shown in Figure 3 (left) representing, respectively,

the proportion of the empty volume to the total volume, the heat generation of the solid part contained inside the porous volume and the pressure loss in the cooling channels. The sum of the energy that is generated in the porous zone and the one that is dissipated from the remaining surfaces of the core and coils is equal to the total power losses of the transformer in the Complete model. The pieces of corrugated cardboard placed inside the channels have been modelled as thermally coupled walls of 1.5 mm of thickness, one-dimensional heat conduction and a thermal conductivity of 0.45 W/m·K. The surfaces of the casing (the lid, all the vertical surfaces and the base, with respective thicknesses of 6 mm, 1.2 mm and 5 mm) are modelled as solid walls with one-dimensional heat conduction and a thermal conductivity of 50 W/m·K. In the outer side of these external walls, depending on the zone, convective or mixed (convection and radiation) boundary conditions are considered as it can be seen in Table 3.

4.5. Discretization and Resolution

The *Finite Volume Method (FVM)* is applied to discretize the differential equations of the mathematical model described above, using a segregated implicit solver to solve the generated algebraic equation system. Therefore, equations are linearised and then sequentially solved using the Gauss-Seidel algorithm accelerated by an Algebraic Multigrid method [18]. The pressure-velocity coupling is achieved through the use of the *SIMPLE* algorithm [19]. Diffusive terms of the equations are discretized using a second-order centred scheme, and the convective terms are discretized using a second-order upwind scheme [17]. A body force weighted scheme [20] is chosen in the discretization of pressure to deal with this buoyancy-driven flow. All this numerical procedure has been implemented in the unstructured *CFD* code Fluent V.6.3 [21].

4.6. Convergence Criteria

Three main convergence criteria have been applied to determine when the numerical procedure described in the previous paragraph has converged to a solution. The first criterion consists of reaching stable values for the temperatures at all the surfaces of the transformer, meaning that a converged steady state has been reached (a variation of less than 0.5 °C in 1000 iterations is required). The second criterion is the balance between the energy losses from the internal surfaces of the transformer and the energy that is dissipated through the external surfaces by convection and radiation (a difference of less than 1% is required). The final criterion is to check that the values for the scaled residuals of the equations are below

certain magnitudes (10^{-3} for the mass, momentum and turbulent equations and 10^{-6} for the energy equation).

5. VERIFICATION AND VALIDATION

The following procedure has been applied to be sure of a correct verification and validation of the proposed Slice model: Firstly, the results of the Complete and Slice models are compared checking equivalent flow and thermal performances. After this the attention is focused exclusively on the Slice model and the adequateness of different turbulence models and near-wall approximations is checked. In a subsequent step, grid independence of the obtained results is verified taking into account that meshing requirements are lower in the Slice model than in the Complete model. Lastly, an analysis of the different thermal boundary conditions that have been tested is shown. The final Slice model will be validated taking into account various experimental measurements that have been previously carried out.

5.1. Complete vs. Slice Model

As has been pointed out in a previous section, the high computational resources that the Complete model requires makes it cumbersome to work with, to verify and validate, and to analyse its results. These tasks have only been carried out for the Slice model and are described in the following sections.

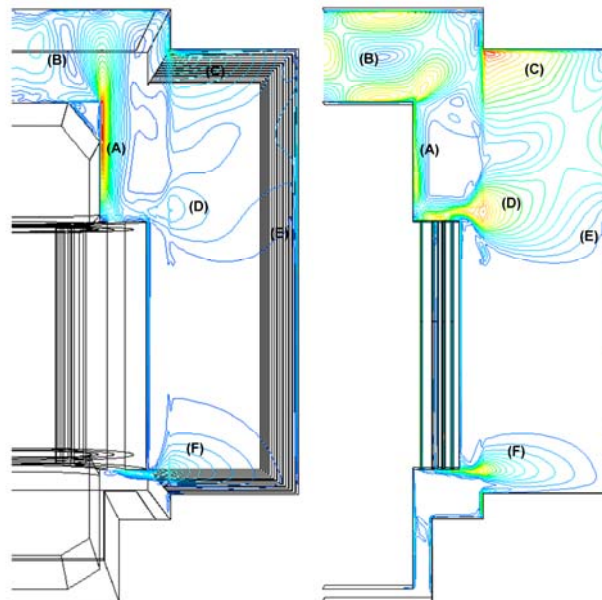


Figure 4 Oil flow patterns in a vertical mid-plane of one central fin for *Transf-02*: Complete (left), Slice (right).

The Complete model is compared to the Slice model to check if the oil flow pattern and the oil temperature distribution are similar in both models, not being influenced by their particular geometry. It is known from Fig. 2 that the Complete model only covers a portion of it, being more of a two dimensional kind.

Tale 4 Numerical temperature results of the Complete and Slice models and differences between them.

	<i>Transf-01 (P_{N,1})</i>			<i>Transf-02 (P_{N,2})</i>		
	<i>Complete</i>	<i>Slice</i>	<i>Dif.</i>	<i>Complete</i>	<i>Slice</i>	<i>Dif.</i>
$T_{ambient}$ (°C)	25		-	25		-
ΔT_{oil} (°C)	64.6	66.0	-1.4	51.2	52.6	-1.4
ΔT_1 (°C)	60.0	61.2	-1.2	46.8	49.0	-2.2
ΔT_9 (°C)	62.6	63.7	-1.1	49.5	50.9	-1.5
ΔT_{10} (°C)	62.3	63.2	-0.9	48.8	50.3	-1.6
ΔT_{11} (°C)	61.2	62.1	-0.9	47.5	48.6	-1.1
ΔT_{12} (°C)	61.2	62.1	-0.9	47.4	48.8	-1.3
ΔT_{13} (°C)	59.1	58.7	+0.4	44.6	43.0	1.6
ΔT_{14} (°C)	59.0	58.6	+0.4	44.4	42.8	1.6
ΔT_7 (°C)	49.8	28.5	+21.3	35.6	17.4	+18.3

Table 4 presents surface temperature differences between the Complete and Slice models for two different transformers (*Transf-01* and *Transf-02*) under the same basic boundary conditions. A thermal resemblance between both models can be ascertained, with temperature differences on the external surfaces that have higher heat dissipation (central fins and lid), to the order of 1-2 °C. A bigger difference of 15-20 °C is observed at the base of the models due to inevitable meshing limitations for the Complete model in the lower cold zone. In fact, both models predict correctly the experimentally observed thermal stratification of the oil inside the casing. The Slice model doesn't include the real physical position of the oil probe inside the transformer as in the Complete model because the oil probe is located under a corner of the lid [2, 3]. But taking into account the thermal stratification that has just been mentioned, it can be considered that oil temperatures remain practically equal if the vertical position of the measurement point is the same in both models. Figure 4 shows that the obtained oil flow patterns, especially in the hollow fins, are very similar in both models. The oil flow patterns will be fully explained and described in a subsequent section.

The Complete model shows some secondary details, such as some higher local thermal variations on the lid and the fact that the average temperature on the external fins is a little bit lower than on the central fins, which obviously cannot be reproduced by the Slice model.

All these data and observations guarantee that, by using the Slice model, appreciable computational resources can be saved without losing essential details of the entire cooling phenomena, and illustrates the validity of the first modelling hypothesis. In the following sections only the Slice model is analysed, searching for the most adequate modelling features.

5.2. Turbulence Models

Turbulence has been modelled using well known two-equation models, obtaining in the process numerical results for the mean flow variables. These turbulence models have not been specifically developed to study natural convection because they consider, following the original Boussinesq hypothesis, an isotropic relation between temperature gradients and turbulent heat fluxes in conjunction with a constant turbulent Prandtl number that relates the turbulent eddy and thermal diffusivity. Nevertheless, they have been chosen for their simplicity, efficiency and extensive use in a wide variety of industrial applications [22], showing good results in the present case too.

After an initial evaluation, the use of simplified *Wall Functions* has been discarded due to inaccuracies in the predicted heat transfer values, and a resolution procedure up to the wall has been adopted. Several turbulence models have been tested, paying special attention to those with different treatment of the Low Reynolds Number effects near the walls: the *Renormalisation Group (RNG) $k-\epsilon$* model [15] with a *2-Layer* approximation close to the walls [16], and several *Low Reynolds $k-\epsilon$* models like *Abid* [23], *Launder-Sharma* [24] and *Chang-Hsieh-Chen* [25]. The results of the oil flow patterns and thermal performances, including external surface temperatures and heat fluxes, are quite similar for all of them. The temperatures with the *RNG $k-\epsilon$* turbulence model are a little bit higher but they also show a higher vertical variation. This fact fits better with the higher vertical thermal variations that have been experimentally observed on the fins as shown in Figure 8. If the top oil temperature obtained for *Transf-01* applying this turbulence model is taken as a reference for comparative purposes, the temperature difference with the *Abid* case is of -0.98 K, with the *Launder-Sharma* case of -2.16 K, and with the *Chang-Hsieh-Chen* case of -1.98 K. Taking into account the observed performances, the *RNG $k-\epsilon$* model

with the *2-Layer* approach close to the walls has been considered as the most suitable option taking into account its better numerical behaviour.

5.3. Grid Independency

The grid independency of the results of the Slice model is checked by means of the so called Grid Convergence Index (*GCI*), based on the Richardson Extrapolation method [26]. This value is used to determine the discretization error by comparing the results for three different meshes. The first case (N_1 : 600,000 elements) is the coarser one, the second case (N_2 : 1,170,000) represents an intermediate grid level and the third case (N_3 : 2,320,000) is for the finest mesh. A constant and structured 3D refinement factor has been maintained with a value of 1.25.

As the main interest is focused on the thermal results, mean surface temperature values of *Transf-01* have been used as control parameters in the evaluation of the discretization error. The maximum *GCI* value found is of about 0.35% in the intermediate-grid solution and of 0.1% in the fine-grid solution showing a good asymptotic behaviour at most checked temperatures. The local apparent order of accuracy p ranges from 3.07 to 8.95 for all the verified values. If the top oil temperature is taken as reference, results are quite invariable as well, showing even lower *GCI* values. These results show that the assumed discretization error should be low enough if an intermediate (N_2) grid level is chosen for the Slice model.

5.4. Evaluation of Thermal Boundary Conditions

One of the most important and critical parts of the development of a mathematical model is the determination of the values for the boundary conditions. For most of the mathematical models of industrial real systems their values cannot be easily established and a further evaluation is required to set them up properly. For the oil flow inside a transformer, a previous work presented in [27] showed the importance of a precise characterisation of the thermal boundary conditions (*TBC*) to obtain acceptable results. In the present paper, a broader analysis concerning to the *TBC* is done.

Constant and uniform heat fluxes are imposed on the internal surfaces of the models, representing the heat generation and the anisotropic heat conduction inside the core and the several zones in which the LV and HV coils are divided by the cooling channels. Equations (6) to (8) shows that these heat fluxes are calculated dividing the power value that correspond to each solid portion inside the transformer by its total surface area (A_{Core} , $A_{i,LV}$ and $A_{i,HV}$). $P_{N,Core}$, $P_{N,LV}$ and $P_{N,HV}$ are experimentally known power values

(standardised power measurements of the heat losses of the core, the LV and HV coils as described in [1]) and $Vol_{i,LV}$ and $Vol_{i,HV}$ represent the volume of copper contained in each portion of the LV or HV windings. The sum of these volumes gives the total volume of copper in the windings, which can be divided in $Vol_{Tot,LV}$ and $Vol_{Tot,HV}$. During the experimental campaign no internal surface temperatures could be measured because commercial transformers were used, making it impossible to evaluate the adequateness of this common approximation (second modelling hypothesis). Nevertheless, taking into account the thermo-electrical phenomena that are generating heat losses homogeneously in the solid volume (sheets of steel in the core and wires of copper in the coils) this solution can be logically assumed.

$$\text{Core} \quad q_{Core}'' = \frac{P_{N,Core}}{A_{Core}} \quad (6)$$

$$\text{LV Coils } (Vol_{i,LV}) \quad q_{i,LV}'' = \frac{P_{N,LV} \cdot \left(\frac{Vol_{i,LV}}{Vol_{Tot,LV}} \right)}{A_{i,LV}} \quad (7)$$

$$\text{HV Coils } (Vol_{i,HV}) \quad q_{i,HV}'' = \frac{P_{N,HV} \cdot \left(\frac{Vol_{i,HV}}{Vol_{Tot,HV}} \right)}{A_{i,HV}} \quad (8)$$

Following the third modelling hypothesis, two different heat transfer phenomena have to be described on the outer surfaces of the Slice model: convective heat transfer with the air and radiation heat exchanges with the surroundings. The first one is going to be expressed by means of correlations between a mean or local *Raleigh* number (Ra , Ra_y) and a mean or local *Nusselt* number (Nu , Nu_y) as is explained later. The radiation heat exchange can be easily stated in open zones such as the lid or the base. It has been assumed that these surfaces exchange radiation with black body surroundings at ambient temperature, except for the ground where a measured temperature is considered. In the vertical region surrounded by the fin arrangement, the net value of heat exchanged by radiation is relatively small compared with the convective one, in fact, only on the more exposed extremes of the fins is it relevant. In this region, the radiation will be introduced by means of a mixed heat transfer coefficient.

In a first approach, an estimation of constant mean heat transfer coefficients was done based on measured surface temperatures and convective correlations from bibliography [28] and the radiation was dismissed in the vertical zone of the transformer between fins. For example, in the case of *Transf-01*, a mean value of $h = 4.88 \text{ W/m}^2\cdot\text{K}$ was used on the fins taking ambient temperature as a reference for air temperature. Unfortunately, this supposition led to insufficient heat dissipation on the fins as can be

deduced from the very high differences in temperature values in Table 5 (d). An unacceptable difference of 11.3 °C is found in the top oil temperature, and the discrepancies are considerably higher in the lower part of the model. In Figure 8 it can be ascertained that experimental surface temperature variations on the fins are higher in the vertical direction than in the horizontal one. These facts indicate that at least a vertical variation of the boundary conditions is needed by the model to work properly, while a horizontal variation does not seem so critical. On the other hand, the mean heat transfer coefficient values that have been used in horizontal places like the lid and the base seem to be valid because the obtained temperature distributions are always more uniform.

As a second step, a sensitivity analysis was performed to calibrate the influence of relative changes on external *TBC*. Three different parameters were independently varied on the *TBC* for the lid, base and fins: the external heat transfer coefficient (h), the reference ambient air temperature (T_{amb}) and the external black body temperature for radiation heat exchanges (T_{rad}). Variations of $\pm 50\%$ were adopted for these parameters. In the case of h the percentage was directly applied, and in the case of both temperatures, a variation of the relative temperature with respect to a reference temperature was used, following equation (9). Only the influence of all these variations in the top oil temperature of *Transf-01* is shown for brevity.

$$T_{x,New} = T_{ref} \pm 1.5 \cdot (T_{x,Old} - T_{ref}) \quad (9)$$

The Slice model has proved to be very sensible to variations of the *TBC* on the fins due to the concentration of the dissipation area in that zone. If the attention is focused on that region, a great non-linear variation of -11.4/+22.0 K is obtained for modifications of h . Another considerable variation of +5.9/-6.3 K appears if T_{amb} is changed. The changes are relatively small if the *TBC* of the lid are varied (-0.9/+1.1 K for h and +0.1/-0.2 K for T_{amb}) and practically inappreciable if the base is touched. The influence of the radiation is only relevant if the upper black body temperature is changed for the lid. Nevertheless, a limited variation of only +0.6/-0.9 K is observed. In summary, these values show again that special care is needed in the treatment of *TBC* of the fins.

Following this, an auxiliary differential mathematical model representing the air movement between the external surfaces of two adjacent fins of *Transf-01* was developed to study the heat transfer process that takes place there. The main utility of this auxiliary model is to obtain a more realistic external *TBC* for the Slice model, especially for all the vertical surfaces where higher temperature and heat flux

variations have been observed. A fully detailed description, verification and validation of this auxiliary model are outside the scope of the present paper, but all the main aspects will be shown.

The geometry of this model can be considered as the negative portion of the Slice model geometry for *Transf-01*, containing the air surrounding a unique hollow fin. The internal limits of the auxiliary model are the external limits of the Slice model that can be seen in Fig. 3 (right). Three different surface temperature distribution maps, based on the measured temperature values for the three power cases of *Transf-01*, are imposed as boundary conditions in these internal limits. The external limits are the ground, where constant and measured temperatures have been imposed, and the upper and lateral air limits located at a distance of 1.5 m from the surfaces of the casing. Atmospheric pressure and measured ambient temperatures have been used as boundary conditions in these limits.

The Ideal Gas equation is used to model the variation of the density of the air with the temperature, the rest of the properties being temperature dependent as well [28]. The radiation heat exchange is considered by means of the *Discrete Ordinates (DO)* model [29] which is solved once every ten ordinary iterations. It has been assumed that the air does not participate in the radiation and that the different surfaces in the domain are gray and diffuse. The same turbulence model as in the Slice model has been used taking into account that natural convection is involved once again.

The resolution procedure and convergence criteria are conceptually the same as in the Slice model. The validity of the auxiliary air model is checked by comparing the power value fraction dissipated from the surfaces of the casing with the experimentally measured power losses, obtaining acceptable differences of only -2.7% for the $P_{N,1}$ case (-1.6% for $\frac{3}{4} P_{N,1}$, and 0.3% for $\frac{1}{2} P_{N,1}$). Air temperatures have been checked additionally at the outlet of the fins obtaining once again satisfactory results: a difference of -1.8 K for the $P_{N,1}$ case, -0.3 K for $\frac{3}{4} P_{N,1}$ and +1.2 K for $\frac{1}{2} P_{N,1}$.

Figure 5 shows the Nu_y vs. Ra_y curves that have been obtained over the vertical line located in the middle of the lateral surface of the fins as shown in Fig. 2. The correlation that can be extracted from these curves represents exclusively the heat that is dissipated by means of convection in a centred line of the fins and its vertical variation. It has been calculated that an additional 8% of heat is dissipated by convection if horizontal variations are taken into account in the auxiliary air model. This effect is focused on the external lower corner of the fins. An extra 12% of heat is dissipated by means of radiation between the fins and the surroundings if this simplified convective heat transfer is taken as a reference again.

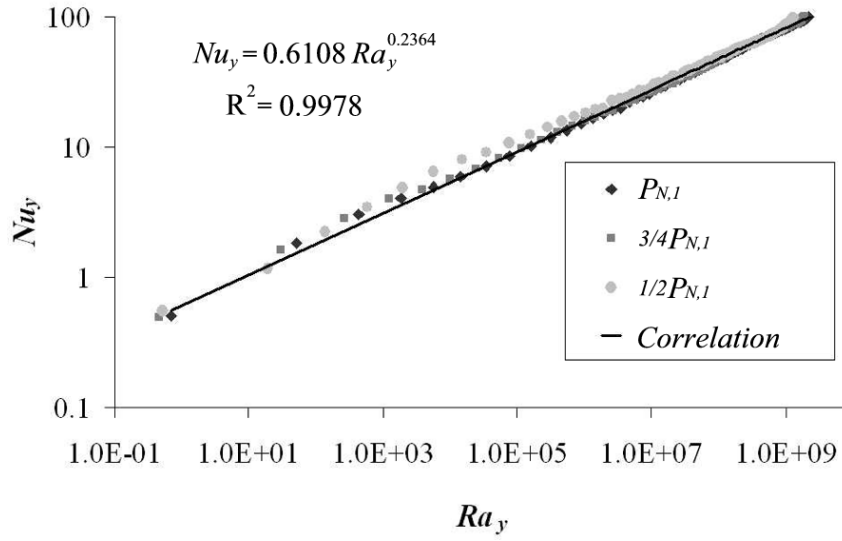


Figure 5 Nu_y vs. Ra_y for the air on the vertical line in the middle of the lateral surface of a fin.

Returning to the Slice model, the convective heat transfer correlation for vertical zones shown in Figure 5 is multiplied by a constant value of 1.22 to take into account these effects, in a mixed way. Bibliographical heat transfer correlations [28] have been maintained in the remaining zones. Equations (10) to (13) are the final *TBC* that will be used in the devised Slice model. The selection and calibration of these simplified external *TBC* has been done taking into account their later use on the simplified algebraic zonal model that is being developed based on the results of the differential numerical model analysed in the present paper. This model only considers vertical thermal variations in the fins according to the experimental results (Table 2) where the horizontal temperature gradients are negligible compared to the vertical ones.

$$\mathbf{Lid} \quad \left\{ \begin{array}{ll} \text{If } Ra_L < 10^7: & \overline{Nu}_{Lid} = 0.865 \cdot Ra_L^{0.25} \quad (10) \\ \text{If } Ra_L > 10^7 & \overline{Nu}_{Lid} = 0.24 \cdot Ra_L^{0.333} \quad (11) \end{array} \right.$$

$$\mathbf{Base} \quad \text{All } Ra_L \quad \overline{Nu}_{Base} = 0.27 \cdot Ra_L^{0.25} \quad (12)$$

$$\mathbf{Vertical (Fins)} \quad \text{All } Ra_y \quad Nu_y = 1.22 \cdot (0.6108 \cdot Ra_y^{0.2364}) \quad (13)$$

where:

$$Ra_L = \frac{g \cdot \beta \cdot (T_s - T_{amb}) \cdot L^3}{\nu \cdot \alpha} \quad (14)$$

$$Ra_y = \frac{g \cdot \beta \cdot (T_{s,y} - T_{amb}) \cdot y^3}{\nu \cdot \alpha} \quad (15)$$

All the air properties are calculated at the film temperature, except for eq. (13) where they are calculated at the ambient temperature. The value of the different heat transfer coefficients that are obtained with these equations depends on the effective value of T_s , which is a result of the simulation. This fact introduces an additional non linearity in the Slice model because TBC will change after each iterative step.

Table 5 Numerical temperature results of the Slice models and differences with experimental results (from Table 2).

	<i>Transf-01</i>								<i>Transf-02</i>		<i>Transf-03</i>	
	$P_{N,1}$		$P_{N,1}$		$\frac{3}{4} P_{N,1}$		$\frac{1}{2} P_{N,1}$		$P_{N,2}$		$P_{N,3}$	
	<i>Model</i> ^(d)	<i>Dif.</i>	<i>Model</i> ^(e)	<i>Dif.</i>	<i>Model</i> ^(e)	<i>Dif.</i>	<i>Model</i> ^(e)	<i>Dif.</i>	<i>Model</i> ^(e)	<i>Dif.</i>	<i>Model</i> ^(e)	<i>Dif.</i>
ΔT_{oil}	62.7	11.3	53	1.6	42.8	1.0	31.7	0.2	49	2.4	56.7	0.5
ΔT_1	57.8	11.0	48.1	1.3	38.1	-0.2	27.3	-2.1	45.3	-0.8	51.4	-2.2
ΔT_9	60.5	11.0	50.6	1.1	40.6	0.1	29.7	-0.8	47	0.1	54.2	-0.3
ΔT_{10}	59.9	12.8	50	2.9	40	1.4	29.3	0.4	46.4	2.1	53	3.6
ΔT_{11}	58.8	14.0	48.3	3.5	38.3	1.9	27.8	0.9	44.6	1.5	50.7	5.9
ΔT_{12}	58.8	14.4	48.4	4.0	38.4	2.4	27.8	1.1	44.7	2.7	50.8	6.9
ΔT_{13}	57.4	21.6	42.1	6.3	32.5	3.9	22.4	2.1	36.4	4.7	42.5	7.6
ΔT_{14}	55.3	21.1	41.9	7.7	32.3	5.1	22.3	2.7	36.2	5.5	41.5	8.9
ΔT_7	25.6	12.4	13.4	0.2	10.7	-0.5	8.1	-0.3	15.2	-3.9	23.8	4.1

(d) External TBC : Constant (it is an initially fixed value) and Uniform (it does not depend on geometrical coordinates).

(e) External TBC : Non-Constant (it changes after each iteration) and Variable (in the vertical direction).

Table 5 (e) contains all the temperature results obtained with the final Slice model for different transformers and power losses. The temperature results of the model are always slightly higher than the experimental ones. Differences with experimentally measured values are small at the upper zone of the model, especially for the top oil temperature where a maximum discrepancy of 2.4 °C is obtained only for *Transf-02*. The sensitivity of the vertical temperature variation has been improved considering a vertical variation of the TBC , but differences are still appreciable (up to 9 °C for the worst case) at the lower external zone of the fins, T_{14} . The reason for this fact is that, in the Slice model, the mixed heat transfer coefficient over the fin surfaces is only dependent on the vertical coordinate, not on the horizontal one, and that in reality the radiative heat exchange is a phenomenon focused at the extremes of the fins. Either way, the averaged error of about +3 K that appears on the fins with these simplified TBC can be assumed, validating the results of the Slice model for diverse transformers and power losses.

6. RESULTS AND DISCUSSION

Meaningful and novel information has been obtained concerning the physical phenomena that govern the cooling of *ONAN* distribution transformers using the developed, verified and validated Slice model. These results are going to be briefly analysed from the point of view of flow patterns and thermal distributions. *A priori* it could be thought that the performance of the oil inside a distribution transformer is equal to that found inside a simple closed cavity with differentially heated vertical walls [30]; that is, the oil moves up and down exclusively due to thermal differences in a natural convection movement. The present model predicts that there are some additional effects influencing the global oil movement, especially in the hollow fins.

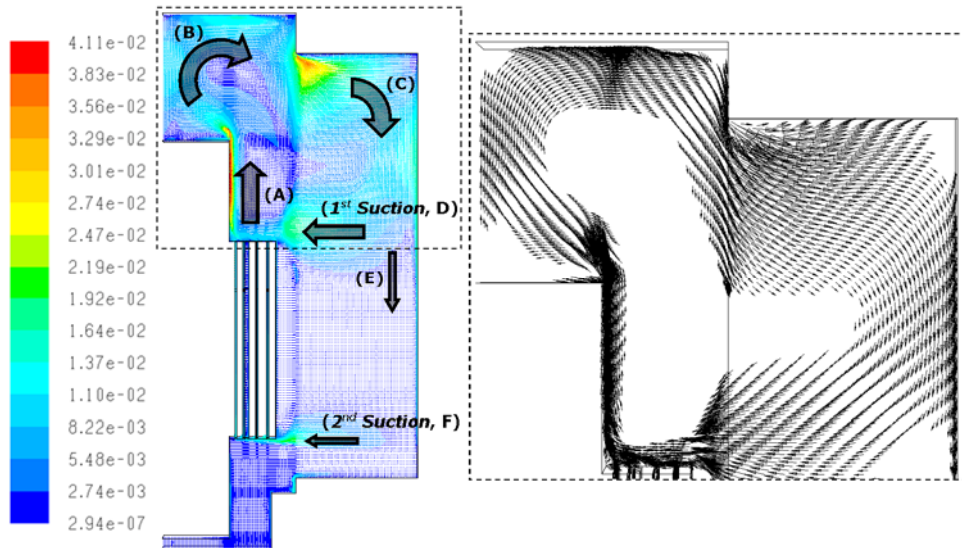


Figure 6 Results of Velocity Vectors in a vertical mid-plane of the fins of *Transf-01* (in m/s).

Almost the same flow pattern that has been sketched previously in Fig. 4 for *Transf-02* can be observed in Figure 6, where the velocity vectors in the mid plane of the Slice model for *Transf-01* are represented. This characteristic oil movement, which has been stressed using arrows in Fig. 6, is common for all the studied transformers. The oil mass flows increase with the vertical coordinate because convective boundary layers are being generated in the presence of internal hot walls. At the bottom of the transformer the temperatures are relatively low and the oil movement is inappreciable. The movement is focused on the upper hot zone of the model, close to the walls, while in the central zones oil is always more static. A notable rising plume is generated close to the upper vertical wall of the core, at the outlet

of the channels (A). This main oil flow rises up to the top part of the domain where it is deflected by the lid and redirected to the fins (B).

Oil flow inside the hollow fins is clearly influenced by their relative position to the coils. The movement is very active again in the upper part and decreases when the oil moves down. The main oil flow enters the hollow fins from the highest zone of the casing (C). When it arrives up to the height of the upper zone of the coils, flux is divided into two parts. A fraction (*1st Suction*, D) is redirected to the outlets of the coil channels and exits the hollow fin. The other fraction (E) moves down and exits at the height of the bottom inlets of the coil channels (*2nd Suction*, F). These special horizontal flow movements are equally predicted by the Complete model and they appear to maintain a zonal momentum and mass balance with the oil getting in to and out of the coil channels. So, they can be considered as an indirect effect of the principal buoyant forces that are generated in the proximities of the principal heat sources. The mass flow that is involved in the *1st Suction* is going to be compared for different transformers and power losses as a reference. For *Transf-01* values of 3.60 g/s, 5.39 g/s and 8.31 g/s can be found as power losses increase. For *Transf-02* a value of 5.21 g/s is obtained and for *Transf-03* a value of 4.97 g/s.

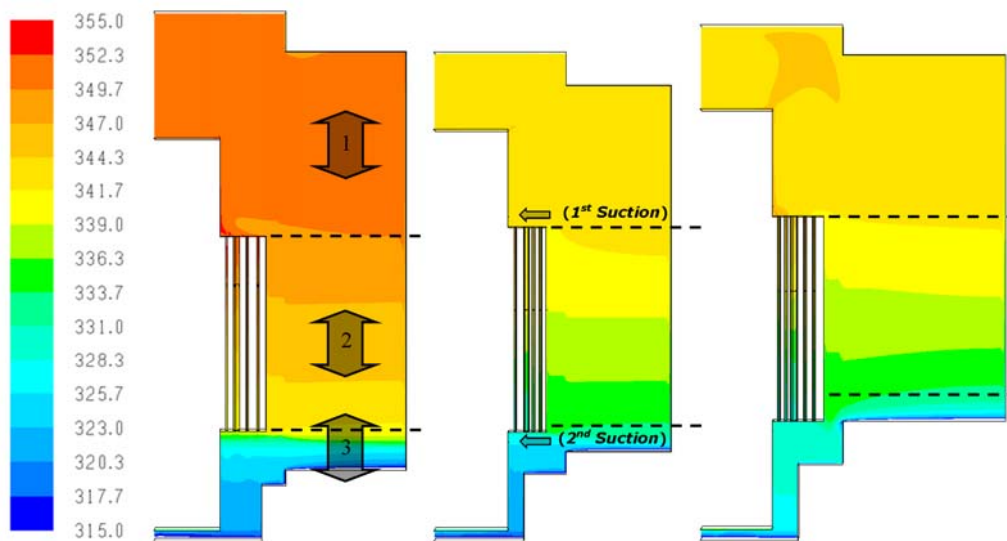


Figure 7 Results of Oil Temperature in a vertical mid-plane of the fins (in K): *Transf-01* (left), *Transf-02* (middle), *Transf-03* (right).

The thermal stratification that is typical in this type of cavity is reproduced in this closed model too, as can be seen in Figure 7. Focusing the attention again on the fins, it can be concluded that the oil temperature is almost uniform in the hollow fin over the *1st Suction* (zone 1), then it decays lineally

between the 1st and the 2nd Suction (zone 2) and, finally, the temperature drops sharply at the bottom part of the fins (zone 3). Thus, the suction phenomenon that has been observed with the Slice model involves a higher vertical thermal variation, which fits better with the experimental observations shown in Fig. 8.

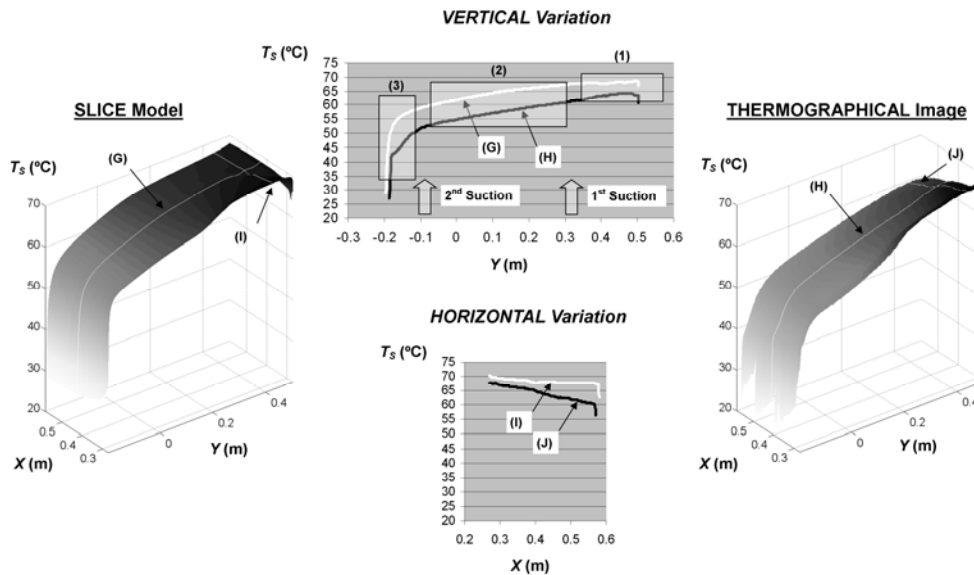


Figure 8 Surface temperature distribution over a fin for *Trans-03*: Simulation result (left), Processed thermographical image (right), Vertical variation (middle, up), Horizontal variation (middle, down).

The special movement of the oil inside the hollow fins will affect the vertical and horizontal thermal gradients of the external fin surfaces and, subsequently, the heat flux distribution. The model predicts a total heat flux distribution that is bigger on the bottom part of the fins and that decays following a potential curve up to the top part. In Figure 8 the surface temperature distribution obtained over the central fin of the Slice model for *Transf-03* is compared with that experimentally measured using thermographical capture on an extreme fin. The comparison between these two temperature distributions can only be made qualitatively, because the extreme fins are always colder than the central fins. Taking this into account, an acceptable resemblance between them can be noticed: the vertical variation is very well reproduced by the Slice model as shown in Fig. 8 (middle, up). Fig. 8 (middle, down) illustrates that the model is less sensible to horizontal temperature variations because the imposed *TBC* only varies in the vertical direction. As has been argued before and shown in Fig. 8, the horizontal temperature variation is clearly less relevant in magnitude than the vertical one.

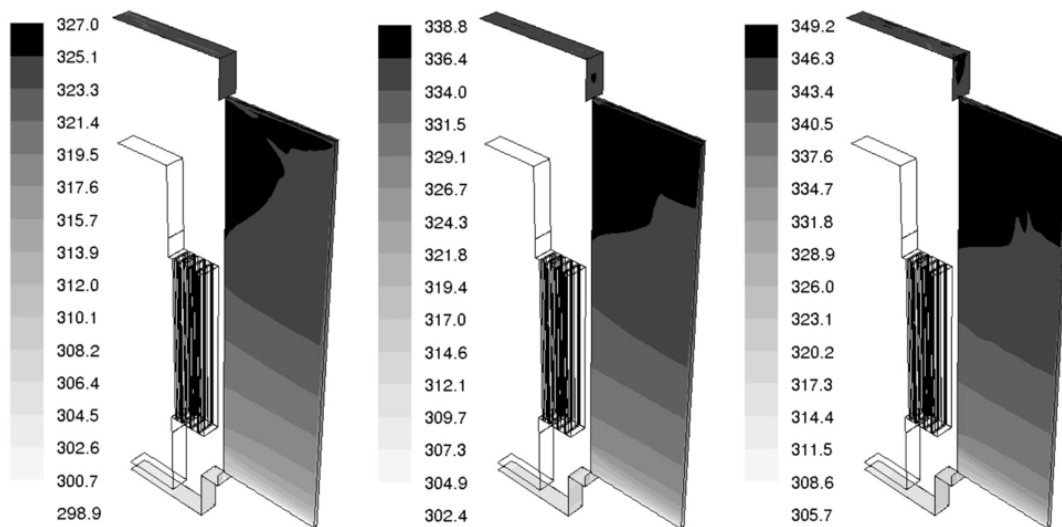


Figure 9 Results of Surface Temperatures on *Transf-01* (in K): $\frac{1}{2} P_{N,1}$ (left), $\frac{3}{4} P_{N,1}$ (middle), $P_{N,1}$ (right).

Attending to Figure 9, where external surface temperatures are showed for diverse power losses of *Transf-01*, a temperature difference of 38.9 K exists in the vertical direction of the model between the top and bottom edges of the fins (32.2 K for $\frac{3}{4} P_{N,1}$ and 24.2 K for $\frac{1}{2} P_{N,1}$). This variation is of about 32.9 K for *Transf-02* and 36.6 K for *Transf-03*. This magnitude is univocally related to the power value managed by the transformer and the length of the fins. On the other hand, as supposed, surface temperatures can be regarded as uniform on horizontal places.

The qualitative and quantitative results of oil flows and temperature distributions shown and discussed in the former paragraphs can be used to analyse and optimise the cooling of *ONAN* distribution transformers by means of design improvements. This information will prove to be instrumental in developing a simplified zonal thermal model of the cooling of *ONAN* distribution transformers in the future. The applicability of the advantageous Slice model idea is obviously restricted to distribution transformers where the oil is moved by natural convection; and it is especially useful in cases where hollow fins are included in the design. Taking into account that 90% of the electric power delivery market (from medium to low voltages) is dominated by this kind of device, the interest of such a tool is remarkable.

7. CONCLUSIONS

A computationally efficient model to represent the thermal performance of an *ONAN* distribution transformer when is located in open air conditions has been developed and numerically solved using *CFD*

techniques. The influence of turbulence modelling in the model's predictions has been evaluated and the grid independence has been verified. An assessment of the external thermal boundary conditions has been carried out, concluding that the heat transfer coefficients must vary in the vertical direction. With the aid of an auxiliary air model, a general correlation for the external heat transfer coefficient on the lateral surface of the fins has been proposed. The final model has been experimentally validated for three heating tests of the same transformer at different power losses and for two other transformers at nominal power losses.

The developed Slice oil model has shown a good capacity to represent the thermal behaviour of the entire transformer. The maximum difference that has been found in the temperature of the oil probe with the experimentally measured values is less than 2.4 °C. Internal oil flow patterns have been qualitatively described in relation to the thermal stratification that appears in this closed cavity and to the unexpected suction provoked by the oil flowing out from the coil channels. It has been concluded that this suction governs the thermal performance of the transformer. This special feature of the flow was not *a priori* predictable taking into account the usual natural convection movement in differentially heated closed cavities. The present model allows this kind of realistic analysis of physical phenomena that are taking place in the process of transformer heat dissipation.

The oil model has proved to be a useful tool for analysing the thermal design of a distribution transformer. With the information provided by the Slice model a simplified zonal algebraic model is being developed to be used as a design and optimisation tool for transformer manufacturers.

Acknowledgments

The authors of this research work wish to acknowledge Ormazabal Corporate Technology, O.C.T., and the Antonio Aranzabal Foundation – University of Navarra for their economic support and collaboration. The experimental measurements carried out by the technicians José Antonio Parada and Iker Barragán, from O.C.T., are also acknowledged.

References

- [1] IEC 60076-7, Power Transformers Part 7: Loading Guide for Oil-Immersed Power Transformers, IEC Standard, 2005
- [2] IEC 60076-1, Power Transformers Part 1: General, IEC Standard, 2000.
- [3] IEC 60076-2, Power Transformers Part 2: Temperature Rise, 2nd edition, IEC Standard, 1997.

- [4] Z. Radaković, and Dj. Kalić, Results of a Novel Algorithm for the Calculation of the Characteristic Temperatures in Power Oil Transformers, *Electrical Engineering* 80 (3) (1997) 205-214.
- [5] V. Galdi, L. Ippolito, A. Piccolo, and A. Vaccaro, Parameter Identification of Power Transformers Thermal Model Via Genetic Algorithms, *Electric Power Systems Research* 60 (2001) 107-113.
- [6] G. Swift, T. S. Molinski, and W. Lehn, A Fundamental Approach to Transformer Thermal Modeling - Part I: Theory and Equivalent Circuit - Part II: Field Verification, Circuit, *IEEE Transactions on Power Delivery* 16 (2) (2001) 171-180.
- [7] G. Pudlo, S. Tenbohlen, M. Linders, and G. Krost, Integration of Power Transformer Monitoring and Overload Calculation into the Power System Control Surface, *IEEE/PES Transmission and Distribution Conference, Yokohama I* (2002) 470-474.
- [8] E. I. Koufakis, C. G. Karagiannopoulos, and P. D. Bourkas, Thermal Coefficient Measurements of the Insulation in Distribution Transformers of a 20 kV Network, *Measurement* 41 (2008) 10-19.
- [9] Z. Radaković, and S. Maksimović, Dynamical Thermal Model of Oil Transformer Placed Indoor, *CIREN 20th International Conference on Electricity Distribution, Prague* (2009) Paper no. 0304.
- [10] K.-J. Oh, and S.-S. Ha, Numerical Calculation of Turbulent Natural Convection in a Cylindrical Transformer Enclosure, *Heat Transfer – Asian Research* 28 (1999) 429-441.
- [11] J.-M. Mufuta, and E. Van den Bulck, Modelling of the Mixed Convection in the Windings of a Disc-Type Power Transformer, *Applied Thermal Engineering* 20 (2000) 417-437.
- [12] N. El Wakil, N. -C. Chereches, and J. Padet, Numerical Study of Heat Transfer and Fluid Flow in a Power Transformer, *International Journal of Thermal Sciences* 45 (2006) 615-626.
- [13] J. C. Ramos, A. Rivas, and J. M. Morcillo, Numerical Thermal Modelling of the Natural Ventilation of a Half-Buried Transformer Substation using CFD Techniques, *Progress in Computational Heat and Mass Transfer* 2 929-934, Lavoisier, Paris, 2005.
- [14] T. -W. Lee, *Thermal and Flow Measurements*, 25-38, Taylor & Francis Group, New York, 2008.
- [15] D. Choudhury, Introduction to the Renormalization Group Method and Turbulence Modelling”, *Fluent Inc. Technical Memorandum, TM-107*, 1993.
- [16] T. Jongen, and Y. P. Marx, Design of an Unconditionally Stable Positive Scheme for the $k-\epsilon$ and Two-Layer Turbulence Models, *Comput. Fluids* 26 (5) (1997) 469-487.
- [17] S. R. Mathur, and J. Y. Murthy, A Pressure-Based Method for Unstructured Meshes, *Numerical Heat Transfer, Part B: Fundamentals*, 31 (2) (1997) 195-215.
- [18] B. R. Hutchinson, and G. D. Raithby, A Multigrid Method Based on the Additive Correction Strategy, *Numerical Heat Transfer* 9 (1986) 511-537.
- [19] S. V. Patankar, *Numerical Heat Transfer and Fluid Flow*, 126-131, Hemisphere Publishing Corporation, New York, 1980.
- [20] J. H. Ferziger, and M. Peric, *Computational Methods for Fluid Dynamics*, 3rd edition 157-217, Springer-Verlag, Germany, 2002.
- [21] Fluent Inc., 2006, “Fluent 6.3 User’s Guide”, Cavendish Court, Lebanon, NH 03766.
- [22] R. A. W. M. Henkes, and C. J. Hoogendoorn, Comparison Exercise for Computations of Turbulent Natural Convection in Enclosures, *Numerical Heat Transfer – Part B – Fundamentals* 28 (1) (1995) 59-78.
- [23] R. Abid, Evaluation of Two-Equation Turbulence Models for Predicting Transitional Flows, *Int. Journal of Eng. Sci.* 31 (6) (1993) 831-840.
- [24] N. Z. Ince, and B. E. Launder, On the computation of Buoyancy-Driven Turbulent Flows in Rectangular Enclosures, *Int. Journal Heat and Fluid Flow* 10 (2) (1989) 110-117.
- [25] K. C. Chang, W. D. Hsieh, and C. S. Chen, A Modified Low-Reynolds-Number Turbulence Model Applicable to Recirculating Flow in Pipe Expansion, *ASME Journal of Fluids Engineering* 117 (1995) 417-423.
- [26] P. J. Roache, Perspective: A Method for Uniform Reporting of Grid Refinement Studies, *ASME Journal of Fluids Engineering* 116 (1994) 405-413.
- [27] J. Gastelurrutia, J. C. Ramos, A. Rivas, J. Izaguirre, and L. Del Río, Mathematical Modelling and Simulation of Natural Convection of Oil Inside Distribution Transformers”, *13th Int. Conference on Modelling Fluid Flow* 1 599-606, Budapest University of Technology and Economics, Budapest, 2006.

- [28] F. P. Incropera, D. P. De Witt, T. L. Bergman, and A. S. Lavine, *Fundamentals of Heat and Mass Transfer*, 6th edition 559-619, John Wiley & Sons, New York, 2006.
- [29] G. D. Raithby, and E. H. Chui, A Finite Volume Method for Predicting a Radiant Heat Transfer in Enclosures with Participating Media, *Journal of Heat Transfer* 112 (1990) 415-423.
- [30] R. De C. Oliveski, M. H. Macagnan, and J. B. Copetti, Entropy Generation and Natural Convection in Rectangular Cavities, *Applied Thermal Engineering* 29 (2009) 1417-1425.